DEUTSCHES ELEKTRONEN-SYNCHROTRON DESY

DESY 74/20
May 1974

High Energy Electron Scattering from ^{6}Li and ^{12}C

by

F. H. Heimlich
Physikalisches Institut der Universität Freiburg/Breisgau

M. Köbberling, J. Moritz, K. H. Schmidt, D. Wegener and D. Zeller
Institut für Experimentelle Kernphysik der Universität (TH) und des Kernforschungszentrums Karlsruhe

J. K. Bienlein, J. Bleckwenn, H. Dinter
Deutsches Elektronen-Synchrotron DESY, Hamburg

2 HAMBURG 52 · NOTKESTIEG 1

To be sure that your preprints are promptly included in the
HIGH ENERGY PHYSICS INDEX ,
send them to the following address (if possible by air mail) :

DESY
Bibliothek
2 Hamburg 52
Notkestieg 1
Germany

HIGH ENERGY ELECTRON SCATTERING FROM ^{6}Li AND ^{12}C

F.H. Heimlich

Physikalisches Institut der Universität Freiburg/Breisgau

M. Köbberling, J. Moritz, K.H. Schmidt, D. Wegener
and D. Zeller

Institut für Experimentelle Kernphysik der Universität (TH)
und des Kernforschungszentrums Karlsruhe

J.K. Bienlein, J. Bleckwenn, H. Dinter

Deutsches Elektronen-Synchrotron DESY, Hamburg

ABSTRACT

We have measured the spectra of electrons scattered from ^{6}Li and ^{12}C for invariant masses of the hadronic system $W \leq 1.5$ GeV and four momentum transfers in the range $5\ fm^{-2} \leq q^2 \leq 12\ fm^{-2}$. We compared the shape of the spectra with different nuclear models. The Fermi-gas model of the nucleus cannot reproduce the data. A shell model with short-range correlations fits the data with a correlation parameter $q_c \approx 250$ MeC/c. From the absolute cross section the effective number of nucleons was derived for quasi-elastic scattering and found to be compatible with A, whereas the effective number of nucleons derived for the excitation of the $\Delta(1236)$-resonance resulted to 0.6 A.

1. INTRODUCTION

The scattering of high energy electrons from nucleons and nuclei has proven to be a powerful tool in the investigation of the structure of strongly interacting particles and nuclei[1] mainly due to the following three reasons:

- The interaction of electrons with the nuclear charge and current densities is well understood and can be described in terms of quantum-electrodynamics.
- The interaction is relatively weak and the one photon exchange is a good approximation also for light nuclei[2].
- In contrast to the absorption of real photons it is possible to vary the four momentum transfer q^2 and the energy transfer ν independently (with $|\vec{q}| > \nu$).

Detailed and systematic data for the scattering of electrons from protons[3] and weakly bound neutrons[4] are now available, therefore the question of the influence of nuclear matter on the structure of nucleons[5] can be attacked. For primary electrons in the GeV-range there exist only data from a few experiments[6,7] which have been mainly analysed in terms of the Fermi-gas model of the nucleus[8].

The aim of the present experiment on scattering of electrons from ^{6}Li and ^{12}C was a threefold one. From the measurement of the absolute value of the cross section in the region of quasi-elastic scattering we wanted to get information about the form factors of bound state nucleons. Secondly, we aimed to investigate the influence of nuclear matter on resonance excitation. Furthermore, from the shape of the spectra we wanted to get information on the momentum distribution of nucleons bound in ^{6}Li and ^{12}C.

In chapter 2 a short description of the apparatus is given, in chapter 3 data reduction and corrections are discussed. The experimental results are presented in chapter 4 and compared with a Fermi-gas model of the nucleus (4.1) as well as with the shell model nuclear wave functions (4.2). We also compared our data with free electron-nucleon cross sections (4.3) and with deep inelastic electron scattering data from ^{12}C (4.4).

2. APPARATUS

This experiment was performed at DESY Hamburg. A slowly ejected electron beam was focussed on a 0.004 radiation length thick target of ^{6}Li or ^{12}C. The Li-target was enriched to 95.6% ^{6}Li. The intensity of the beam was monitored with a totally absorbing Faraday-cup and a secondary-emission monitor with an accuracy of ±1%. The scattered electrons were detected with a spectrometer which consisted of a bending magnet with a homogeneous field, four wire spark chambers with ferrite-core readout, and scintillation counters, including a shower counter. An additional Cerenkov counter was used to test the pion background. This spectrometer hasthe advantage of having a constant momentum acceptance of ±20%, which allows to measure electron spectra from the quasi-elastic peak up to invariant masses of W = 1.5 GeV with one spectrometer setting. The spectrometer covered a solid angle of 0.69×10^{-3} sr.

The spark chamber readout-system and the electronic counters were connected to a CDC 1700 computer. For each event-trigger, the computer calculated on-line the radius of curvature of each particle passing through the spectrometer magnet. Moreover, the shower spectrum and the energy spectrum of the

scattered electrons were calculated. Thus, the performance of the apparatus was continuously monitored during the run. The whole apparatus is described in detail in refs. 3, 9.

The measurements for ^{6}Li and ^{12}C were performed at different values of the kinematic parameters which are compiled in table 1.

TABLE 1: Kinematic parameters of the experiment.

	E_1 (GeV)	θ_e	q^2_{qel} (fm^{-2})	q^2_{1236} (fm^{-2})
^{6}Li	2.5	12°	6.6	5.6
	2.7	13.8°	10.0	8.7
	2.7	15°	11.6	10.0
^{12}C	2.0	15°	6.6	5.4
	2.5	15°	10.0	8.7
	2.7	15°	11.6	10.0

3. DATA REDUCTION AND CORRECTIONS

Before computing the cross sections from the counting rate, each event was corrected for the momentum acceptance and the scattering angle.

The momentum acceptance of the spectrometer is constant over a broad interval. Only in the low momentum region of the spectrum the acceptance decreases. The corrections due to the momentum acceptance were determined from the data to be less than 30% with an error of ±2%.

Since the scattering angle of each detected electron was measured, the angular dependence of the energy could be taken into account to improve the energy resolution of the spectrometer, yielding $\Delta p/p = 1.2\%$ FWHM for the scattered electrons. This resolution was tested by elastic electron proton scattering[3]. The corrections due to pion background were less than 0.5%. By reversing the field of the spectrometer magnet, a Dalitz-pair contamination of the data set was found to be less than 0.1%.

We applied radiative corrections according to the method of Mo and Tsai[10]. In the case of ^{12}C we have measured three electron spectra at the same electron scattering angle but at different primary energies, permitting us to perform a model independent unfolding of the measured cross sections. For ^{6}Li the radiative corrections were applied to the theoretical cross sections to compare them directly with the measured points. The total systematic error is ±3% for the ^{6}Li and ±5% for the ^{12}C data points. This error was obtained by quadratic addition of the uncertainties from target thickness, beam intensity, counter efficiencies, and, in the case of ^{12}C, radiative corrections.

The measured electron spectra for different kinematic parameters are presented in figs. 1 and 2 for ^{12}C and in fig. 3 for ^{6}Li. A systematic error of ±3% is added quadratically to the statistical errors and included in the error bars.

4. EXPERIMENTAL RESULTS AND DISCUSSION

The measured cross sections for ^{6}Li and ^{12}C are tabulated in refs. 11 and 12 respectively. The electron spectra of figs. 1, 2, and 3 show the prominent quasi-elastic peak and the

peak of the first nucleon resonance. Coherent effects, i.e. elastic electron scattering and level excitation, are negligible for the q^2-region covered by the present experiment[6].

4.1 Comparison of the data with the Fermi-Gas-Model

In the one-photon exchange approximation, the twofold differential cross section for electron scattering on spin 1/2 particles is usually given in the form

$$\frac{d^2\sigma}{d\Omega_e dE_3} = \sigma_{Mott} \{W_2(q^2,\nu) + 2tg^2 (\theta_e/2) W_1(q^2,\nu)\} \quad (1)$$

where σ_{Mott} is the Mott cross section, θ_e is the electron scattering angle, W_1 and W_2 are the structure functions of the nucleons, q^2 is the squared four momentum transfer, and $\nu = E_1 - E_3$ is the energy transfer to the hadronic system.

In the case of the simple Fermi-gas model of the nucleus, Moniz has computed the structure functions W_1 and W_2 for the quasi-elastic peak and for the electroexcitation of the first nucleon resonance[8].

In this model the width of the quasi-elastic cross section is directly proportional to the parameter k_F, the maximum nuclear Fermi-momentum. Fitting the prediction of the Fermi-gas model for the quasi-elastic peak to our ^{12}C data we obtain the value $k_F = (191\pm5)$ MeV/c. This is about 15% smaller than the results from measurements at lower four momentum transfers[13].

Moniz treats the first resonance as a stable particle. In order to take into account the finite width of the resonance, we have folded a relativistic Breit-Wigner shape I(W) into

the resonance cross section[14]:

$$I(W) = \frac{\Gamma(W)}{(W-M^*)^2 + \frac{\Gamma^2(W)}{4}} \qquad (2)$$

with

$$\Gamma(W) = \frac{0.128(0.85\,\frac{p_\pi^*}{m_\pi})^3}{1 + (0.85\,\frac{p_\pi^*}{m_\pi})^2} \qquad (3)$$

W : invariant mass of the hadronic system

$M^* = 1236$ MeV: invariant mass of the resonance

$m_\pi = 134$ MeV: mass of the pion

p_π^* : momentum of the decay pion in the rest frame of the resonance.

The non-resonant background and the contribution of the second resonance were assumed to show the same behaviour as shown by free nucleons, since coherent processes are negligible at four momentum transfers of about 8 fm^{-2}. To fit the non-resonant background, the following polynomial was used

$$\sigma_{nres} = \sum_{i=1}^{N} a_i\,(W - W_{th})^{i\,-\,1/2} \qquad (4)$$

where the square root term $(W-W_{th})^{1/2}$ takes into account the behaviour of the production process at the pion threshold. N=3 gives a sufficient fit and has been used for the analysis of all spectra.

The quasi-elastic contribution σ_{qel}, the resonance distribution σ_{1236}, and the non-resonant contribution σ_{nres} were fitted to the measured cross section from ^{12}C:

$$\sigma_{tot} = A\,\sigma_{qel} + B\,\sigma_{1236} + \sum_{i=1}^{3} a_i (W-W_{th})^{i-1/2} \qquad (5)$$

The parameters A, B, and a_i (i=1,3) were determined by the fit. Fig. 1 shows that the simple Fermi-gas model of the nucleus gives only a very crude description of the shape of the spectrum. Even the relative contribution of resonant and non-resonant electron scattering cannot be determined with sufficient accuracy. The errors of the parameters B and a_i, as determined by the fit, are of the order of 100%.

4.2 Comparison with Shell-Model Calculations

To compare our data with realistic nuclear wave functions, we have calculated the quasi-elastic contribution σ_{qel} by integrating the threefold differential cross section over the angle of the recoil proton.

Assuming the impulse approximation, Devanathan[15] has shown that the momentum distribution $P(\vec{p})$ of the bound state nucleons can be factorized. Thus, this representation of the cross section has the advantage of being independent of a special nuclear model.

It is convenient to start with such nuclear wave functions which describe the low energy nuclear data. Therefore, we used Woods-Saxon shell model wave functions and

$$V(r) = V_o \left[1 + \exp\left(\frac{r-R}{a}\right)\right]^{-1} \qquad (6)$$

to calculate the cross section. The parameters a, R, and V_o were determined from the separation energies and from fits to elastic electron scattering[16].

To take into account the short distance effects in the nucleus, we also used shell model wave functions which were modified by short range nucleon-nucleon correlations. These correlations were introduced into the independent particle model by means of the Jastrow method[17] and parametrized by a definite momentum q_c, which is exchanged between two otherwise independently moving nucleons[18]. In these calculations off-shell effects were neglected and the electromagnetic form factors of free nucleons were used.

For the electroproduction of pions in the region of the first nucleon resonance the model of Gutbrod and Simon[19] has been proven to fit the data for free protons[3] and for neutrons[4] in the kinematic region of this experiment. This model includes resonant and non-resonant contributions. Assuming the impulse approximation, we have folded the cross section σ_o for free nucleons, according to the model of Gutbrod and Simon, with the momentum distribution $P(\vec{p}_2)$ of the nucleons bound in the nucleus[20]:

$$\frac{d^2\sigma}{d\Omega_e dE_3}(E_1,E_3,\theta_e) = \int d^3\vec{p}_2 \cdot P(\vec{p}_2) F(\vec{p}_2) \frac{d^2\sigma_o}{d\Omega_e^* dE_3^*}(E_1^*,E_3^*,\theta_e) \cdot \frac{dE_3^*}{dE_3} \cdot \frac{d\Omega_e^*}{d\Omega_e} \tag{7}$$

The kinematic variables in the rest system of the target nucleon are characterized by an asterisk. By $F(\vec{p}_2)$ we take into account the dependence of the virtual photon flux on the Fermi momentum of the target nucleons.

To derive the momentum distributions $P(\vec{p}_2)$ of the bound state nucleons, the same nuclear wave functions were used as in the case of quasi-elastic scattering.

The contribution of the second resonance σ_{1520} was approximated by a resonance of a Breit-Wigner shape located at W = 1520 MeV.

The sum of the quasi-elastic contribution σ_{qel}, the contribution σ_{1236} for the electroproduction of pions in the region of the first nucleon resonance, and σ_{1520} of the second resonance were fitted to the measured cross sections of ^{6}Li and ^{12}C targets:

$$\sigma_{tot} = A\,\sigma_{qel}(q_c) + B\,\sigma_{1236}(q_c) + C\cdot\sigma_{1520} \qquad (8)$$

The parameters A, B, and C were determined by the fit. A set of five different nuclear wave functions was used to fit the data: a pure shell model wave function without short range nucleon-nucleon correlations (q_c=0) and four wave functions with different correlation parameters (q_c = 200, 250, 300, 350 MeV/c). As demonstrated by figs. 2 and 3, the fermi of the spectra of ^{6}Li and ^{12}C can be reproduced quite satisfactorily with a short range nucleon-nucleon correlation parameter q_c = 250 MeV/c. The χ^2 per degree of freedom is about 1 for this choice of the correlation parameter. The wave function without correlations (q_c=0) gives per degree of freedom a $\chi^2 \approx 4$.

The different contributions to the total cross section have a reasonable shape. Curve (a) in figs. 2 and 3 shows that realistic nuclear wave functions are able to reproduce the total width as well as the tails of the quasi-elastic peak. Furthermore, the contribution in the region of the $\Delta(1236)$ resonance (curve b)), according to the model of Gutbrod and

Simon, is in good agreement with the shape of the measured spectra.

As in quite different experiments, e.g. the absorption of pions and (γ,p)-reactions, which are also sensitive to effects at small nucleon-nucleon distances [21], we have also found the best agreement with our data using nuclear wave functions with a correlation parameter $q_c \approx 250$-300 MeV/c. This general agreement of results derived from different experiments seems to show that one can approximate the short range correlations by the momentum exchange of about 250 MeV/c between the nucleons.

4.3 Comparison of the nuclear cross section with the free electron-nucleon cross section

From the assumption of the impulse approximation, one expects that the nuclear cross section for quasi-elastic scattering and for the $\Delta(1236)$-excitation is given by the incoherent sum of the corresponding proton and neutron cross sections.

To test this we evaluated the effective number of nucleons

$$A_{eff} = \frac{\sigma_{nucleus}}{Z \cdot \sigma_{proton} + N \cdot \sigma_{neutron}} \cdot A$$

in two slightly different methods from that used to fit the cross sections (cf. 4.2). For ^{6}Li we integrated the whole quasi-elastic contribution and divided it by the sum of the Rosenbluth cross section of 3 protons and 3 neutrons, assuming a scaling law, a dipole fit, and $^{22}G_{EN} = 0$. In the same way we integrated the contribution of the $\Delta(1236)$-resonance up to an arbitrarily chosen value of W = 1.46 GeV. For ^{12}C

the normalized theoretical distributions for 6 protons and 6 neutrons were added and fitted to the radiatively corrected experimental points. The nucleus to nucleons-ratios are then given by the weight parameters A and B of formula 8 which were determined by the fit. These two methods are consistent within a few percent.

The dependence of our yield ratios for quasi-elastic scattering

$$\frac{\sigma_{qel}}{Z \cdot \sigma_{el,p} + N \cdot \sigma_{el,n}}$$

upon the squared four momentum transfer q^2_{qel} are presented in fig. 4. In the evaluation q^2_{qel} is taken to be the maximum of the quasi-elastic peak. The error bars include statistical errors, systematical errors, and an estimated uncertainty from the nuclear model, totally ±(8-14%).

In fig. 5 our yield ratios are presented for the Δ(1236)-excitation $\sigma_{1236}/(Z \cdot \sigma_p + N \cdot \sigma_n)$ on ^{6}Li and ^{12}C. In this case the squared four momentum transfer q^2_{1236} is taken at the maximum of the resonance peak. In addition to the errors in the quasi-elastic case an error due to the background uncertainty has been included. The total errors amount to ±(10-15%).

In reference to the quasi-elastic process (fig. 4), our ^{6}Li and ^{12}C data at E_1 = 2.5 and E_1 = 2.7 GeV show satisfactory agreement with the ^{12}C data from Stanfield et al.[6] at 1-4 GeV which were obtained by graphical integration over their quasi-elastic distributions and division by the Rosenbluth cross sections; the errors are estimated to be ±(5-10%).

The general trend is that the ratios are compatible with 1 down to momentum transfers of 5 - 10 fm^{-2}. At smaller q^2_{qel}

a reduction in the nuclear cross section arises compared with the sum of the free nucleon contributions.

The ^{6}Li data of Titov and Stepula[7] at E_1 = 1.18 GeV were derived by a quite different method of analysis. Their ratios are about 0.75 over the whole q^2-region and show no decrease at smaller four momentum transfers.

On the other hand, the ^{12}C cross sections at lower primary energies given by Dementii et al.[24] are equal to the sum of the free nucleon cross sections and decrease only at low four momentum transfers.

A possible explanation of the yield ratio reduction at low q^2_{qel} is given by the Pauli exclusion principle. If the three momentum transfer to a nucleon inside the nucleus would be so small that there is no phase space available for the recoiling nucleon (in terms of the Fermi-gas model, the recoil momentum would lie inside the Fermi sphere) then no quasi-elastic scattering process can occur. This effect has been simulated by a Monte-Carlo-method (dotted curve in fig. 4) for ^{6}Li, assuming a momentum distribution from a shell model with correlations (q_c = 250 MeV/c) as described in section 4.2. The dashed curve has been taken from a calculation of Bernabeu[23] for ^{12}C. The decrease at low q^2 reflects again the Pauli exclusion effects.

A completely different picture is indicated by the yield ratios in the region of the $\Delta(1236)$-resonance (fig. 5). Our data for ^{6}Li and ^{12}C stay at a constant value of 0.64 in the four momentum transfer region 5 fm^{-2} $\leq q^2 \leq$ 11 fm^{-2}, whereas the ^{6}Li data of Titov and Stepula[7], based on a different method of evaluation, give a value of about 0.8 in this kinematic region.

If one takes into account the Pauli principle for the recoiling nucleon from the Δ(1236)-decay (cf. the quasi-elastic case), a rough estimate in our kinematic region yields a cross section reduction of only a few percent.

A possible explanation for the reduction of the yield ratio is the modification of the impulse approximation due to the excitation of resonance states in the nucleus[25]. This cross section correction can have a considerable value (an order of magnitude estimate is ~50%)[26] for ^{6}Li and ^{12}C in our kinematic region.

Dover and Lemmer[27] considered resonant pion-nucleus scattering and obtained a quenching of the effective pion-nucleon coupling constant in a nuclear medium, from which in the case of electroproduction of the Δ(1236)-resonance a reduction of the yield ratio is obtained. Besides this, off-shell effects on the nuclear transition form factors may be of importance.

A modification of the Gell-Mann-Goldberger-Thirring sum rule for real photons by Weise[28] predicts a value of

$$A_{eff} = A^{0.76}$$

in the resonance region. This yields $A_{eff}/A = 0.65$ for ^{6}Li and 0.55 for ^{12}C, which, within the error bars are consistent with our data, although the reduction of the cross section for virtual photons is expected to be less.

4.4 Duality and Sum Rules

Another aspect of these data in the resonance region is their connection to the deep inelastic electron scattering.

In the deep inelastic region the structure function $W_2(q^2,\nu)$ shows scaling behaviour

$$W_2(q^2,\nu) \rightarrow F_2(\omega) \quad \text{for} \begin{cases} q^2 \rightarrow \infty \\ \nu \rightarrow \infty \end{cases} \tag{9}$$

where

$$\omega = \frac{2M\nu}{q^2} \quad \text{and } M \text{ is the nucleon mass} \tag{10}$$

The relation between the scaling function $F_2(\omega)$ and the structure function $W_2(q^2,\nu)$ in the resonance region has been discussed by various authors[29]. We refer here to the duality hypothesis of Rittenberg and Rubinstein[30], who derived the sum rule

$$\int \{\frac{\omega}{\omega''} \nu W_2(q^2,\nu) - F_2(\omega'')\}\, d\nu = 0 \tag{11}$$

with

$$\omega'' = \frac{2\nu + \xi^2}{q^2 + a^2} \qquad \begin{aligned} \xi^2 &= 1.3\ \text{GeV}^2 \\ a^2 &= 0.42\ \text{GeV}^2 \end{aligned} \tag{12}$$

for straight lines in the q^2-ν-plane. This sum rule holds for electron scattering on hydrogen and deuterium[20] in the kinematic region of this experiment.

To compute the scaling function $F_2(\omega'')$ for ^{12}C we have used the data of ref. 31 in the kinematic region where $W_2(q^2,\nu)$ shows scaling behaviour for free nucleons. For ^6Li no data in the deep inelastic region were available. From the data of ref. 31 however, $F_2(\omega)$ can only be derived approximately. The hatched region in fig. 6 shows the interval into which the data of the scaling function fall. The comparison of the resonance data of the present experiment with the scaling function derived from ref. 31 shows that the Rittenberg-Rubinstein sum rule also holds for ^{12}C.

ACKNOWLEDGEMENT

We wish to thank the directors of our institutions for the encouragement of this experiment.

We are obliged to the synchrotron group, the hall-service group and all the technical groups at DESY for their excellent support of this experiment. The assistance of Ing. H. Sindt in constructing, testing, and carrying out the experiment is gratefully acknowledged.

This work was supported by the Bundesministerium für Forschung und Technologie.

REFERENCES

1. G. Jakob, T.A.J. Maris
Nucl. Phys. 31 (1962) 139

2. J. Bleckwenn, S. Hartwig, F. Heimlich, G.Huber, E.Rössle, M. Köbberling, J. Moritz, K.H.Schmidt, D. Wegener, D. Zeller
Verhandl D P G (VI) 9, 186 (1974).

3. S.Galster, G.Hartwig, H.Klein, J.Moritz, K.H.Schmidt W. Schmidt-Parzefall, D. Wegener, J. Bleckwenn
Phys. Rev. D5 (1972) 519

4. J. Bleckwenn, H. Klein, J. Moritz, K.H. Schmidt, D. Wegener
Nucl. Phys. B33 (1971) 475

M. Köbberling, J. Moritz, K.H. Schmidt, D. Wegener, D. Zeller, J. Bleckwenn, F.H. Heimlich
Kernforschungszentrum Karlsruhe, Report KFK 1822 (June 1973)

5. G.E. Brown
Comments Nuclear Particle Phys. 3 (1969) 48 and 3 (1969) 78

6. K.C. Stanfield, C.R. Canizares, W.L. Faissler, F.M. Pipkin
Phys. Rev. C3 (1971) 1448

7. Yu.I. Titov, E.V. Stepula, N.G. Afanasev, R.V. Akhmerov, S.A. Byvalin, A.M. Pilipenko, N.F. Severin, T.V. Smelov
Ukrainskii Fiz. Zh. 17 (1972) 1282

Yu.I. Titov, E.V. Stepula
Yadern. Fiz. 15 (1972) 649
(Sov. J. Nucl. Phys. 15 (1972) 361)

8. E.J. Moniz
Phys. Rev. 184 (1969) 1154

9. S. Galster, G. Hartwig, H. Klein, J. Moritz, K.H. Schmidt, W. Schmidt-Parzefall, H. Schopper, D. Wegener
Nucl. Instr. Meth. 76, (1969) 337

10. L.W. Mo, Y.S. Tsai
Rev. Mod. Phys. 41 (1969) 205

11. F.H. Heimlich
Thesis Freiburg 1973 and
DESY, Internal Report F23-73/1

12. D. Zeller
Thesis Karlsruhe 1973 and
DESY, Internal Report F23-73/2

13. E.J. Moniz, I.Sick, R.R.Whitney, J.R.Ficenec, R.D.Kephart, W.P.Trower.
Phys. Rev. Lett. 26 (1971) 445

14. M. Gourdin, P. Salin
Nuovo Cimento 27 (1963) 193

R.H. Dalitz, D.G. Sutherland
Phys. Rev. 146 (1966) 1180

15. W. Weise
Nucl. Phys. A193 (1972) 625

V. Devanathan
Ann. Phys. (N.Y.) 43 (1967) 741

16. L.R.B. Elton, A. Swift
Nucl. Phys. A94 (1967) 52

17. R. Jastrow
Phys. Rev. 98 (1955) 1479

18. B. Blum
Thesis Erlangen 1972

19. F. Gutbrod, D. Simon
Nuovo Cimento 51A (1972) 602

20. M. Köbberling
Thesis Karlsruhe 1973 and
DESY, Internal Report F23-73/3

21. W. Weise
Phys. Lett. 38B (1972) 301

S.T. Tuan, L.E. Wright, M.G. Huber
Phys. Rev. Lett. 23 (1969) 1[illegible]

L.E. Wright, S.T. Tuan, M.G. Huber
Lett. al Nuovo Cimento I (1970) 253

K. Chung, M. Danos, M.G. Huber
Phys. Lett. 29B (1969) 265

K. Chung, M.G. Huber, M. Danos
Z. Phys. 240 (1970) 195

22. S. Galster, H. Klein, J. Moritz, K.H. Schmidt,
D. Wegener, J. Bleckwenn
Nucl. Phys. B32 (1971) 221

23. J. Bernabeu
Nucl. Phys. B40 (1972) 186

24. S.V. Dementii, N.G. Afanasev, I.M. Arkatov, V.G. Vlasenko,
V.A. Goldshtein, E.L. Kuplennikov
Yad. Fiz. 9 (1969) 241
(Sov. J. Nucl. Phys. 9 (1969) 142)

25. M.L. Goldberger, K.M. Watson
Collision Theory
(J. Wiley and Sons, Inc., New York, 1964), p. 687

26. D.I. Julius
Daresbury Nucl. Phys. Lab. DNPL/R20 (1972) and
private communication

27. C.B. Dover, R.H. Lemmer
Phys. Rev. C7 (1973) 2312

28. W. Weise
Proceedings of the International Conference on Photo-
nuclear Reactions and Applications,
Asilomar, 1973, p. 95

29. E.D. Bloom, F.J. Gilman
Phys. Rev. Lett. 25 (1970) 1140

30. V. Rittenberg, H.R. Rubinstein
Phys. Lett. 35B (1971) 50

31. D.E. Andrews
Thesis Cornell University 1972

FIGURE CAPTIONS

Fig. 1 Double differential cross section for $^{12}C(e,e')$, depending on the energy E_3 of the scattered electrons. E_1 = 2.0 GeV, $\theta_e = 15^o$, squared four momentum transfer on the quasi-elastic maximum q^2_{qel} = 10.0 fm^{-2}.

a. quasi-elastic contribution (ref. 8)

b. $\Delta(1236)$-contribution (ref. 8)

c. second resonance and background

d. sum of the theoretical curves,

The momentum distribution of nucleons is given by the Fermi-gas model with k_F = 191 MeV/c.

Fig. 2 Same parameter as in fig. 1.

a. quasi-elastic contribution (ref. 15)

b. $\Delta(1236)$-contribution (ref. 19)

c. second resonance and background

d. sum of the theoretical curves.

A shell model including short-range nucleon-nucleon correlations is used. The correlation parameter was q_c = 250 MeV/c.

Fig. 3 Double differential cross section for $^6Li(e,e')$, depending on the energy E_3 of the scattered electrons. E_1 = 2.7 GeV, $\theta_e = 13.8^o$, q^2_{qel} = 10.0 fm^{-2}.

a. quasi-elastic contribution (ref. 15)

b. $\Delta(1236)$-contribution (ref. 19)

c. second resonance and background

d. sum of the theoretical curves a.-c., which are folded with radiative corrections.

e. sum of the theoretical curves without radiative effects.

The nuclear model is the same as the one used in fig. 2.

Fig. 4 Ratio of the quasi-elastic yield for ^{6}Li and ^{12}C to the sum of the Rosenbluth-cross sections of the protons and neutrons, depending on the squared four momentum transfer q^2_{qel}. The dotted curve is a Monte-Carlo calculation for ^{6}Li taking into account the Pauli principle, the dashed curve is a calculation for ^{12}C (ref. 23).

Fig. 5 Ratio of the $\Delta(1236)$-resonance yield for ^{6}Li and ^{12}C over the sum of the free nucleon cross section (integrated over the $\Delta(1236)$-resonance), depending on the squared four momentum transfer at the $\Delta(1236)$-peak.

Fig. 6 The structure function $\omega/\omega''\ \nu\ W_2$ for $^{12}C(e,e')$ in the resonance region (this experiment) compared with the scaling function calculated from deep inelastic data (ref. 31).

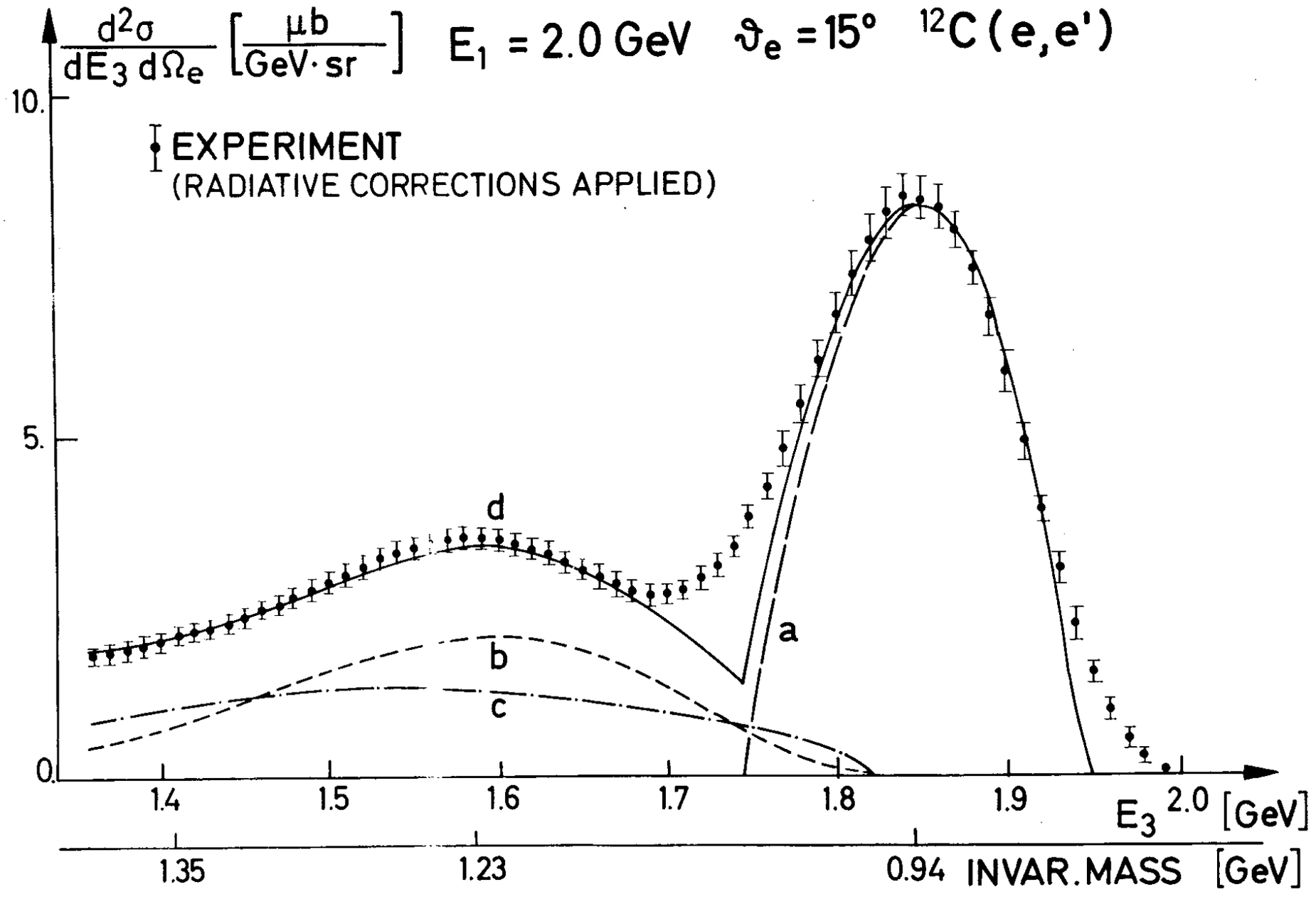
$\frac{d^2\sigma}{dE_3\, d\Omega_e}\left[\frac{\mu b}{GeV\cdot sr}\right]$
$E_1 = 2.0$ GeV
$\vartheta_e = 15°$
$^{12}C(e,e')$
EXPERIMENT
(RADIATIVE CORRECTIONS APPLIED)
10.
5.
0.
d
a
b
c
1.4
1.5
1.6
1.7
1.8
1.9
2.0
E_3 [GeV]
1.35
1.23
0.94
INVAR. MASS [GeV]

FIG.1

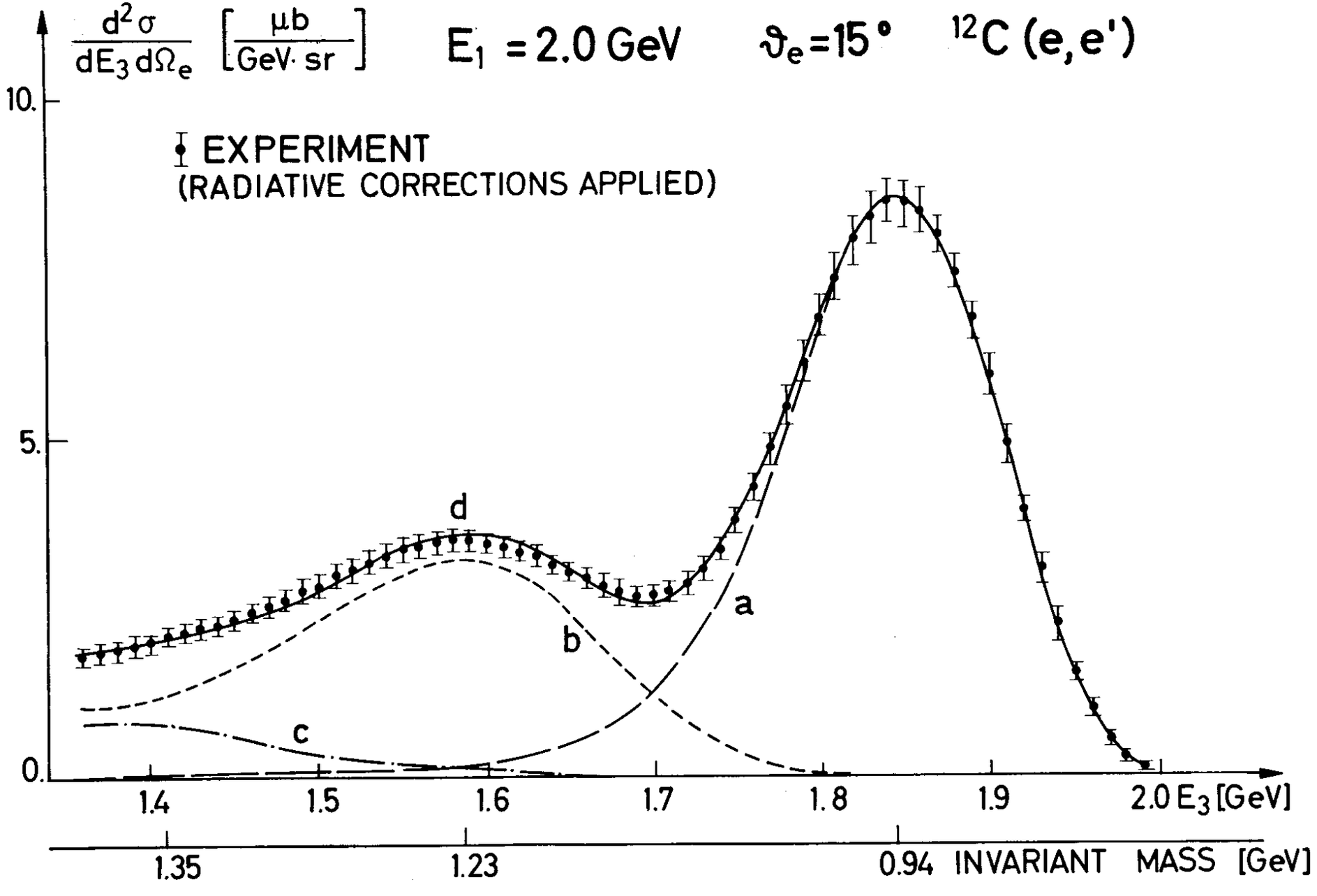
$\frac{d^2\sigma}{dE_3\,d\Omega_e}$ $\left[\frac{\mu b}{GeV\cdot sr}\right]$
$E_1 = 2.0$ GeV
$\vartheta_e = 15°$
^{12}C (e, e')
EXPERIMENT
(RADIATIVE CORRECTIONS APPLIED)
10.
5.
0.
a
b
c
d
1.4
1.5
1.6
1.7
1.8
1.9
2.0 E_3 [GeV]
1.35
1.23
0.94 INVARIANT MASS [GeV]

FIG.2

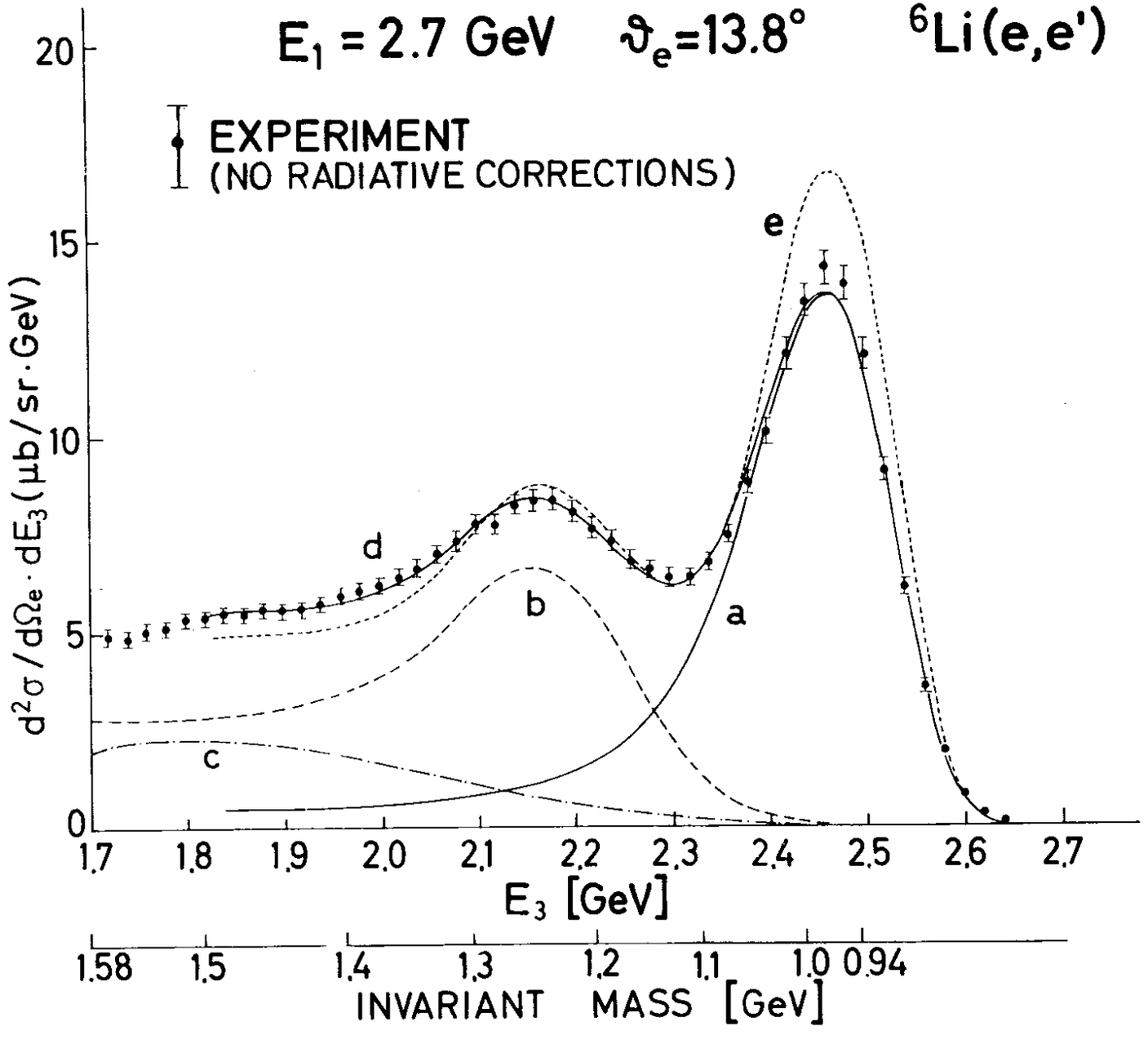
$E_1 = 2.7$ GeV $\vartheta_e = 13.8°$ ^{6}Li(e,e')
EXPERIMENT
(NO RADIATIVE CORRECTIONS)
$d^2\sigma / d\Omega_e \cdot dE_3$ (μb/sr·GeV)
20
15
10
5
0
a
b
c
d
e
1.7
1.8
1.9
2.0
2.1
2.2
2.3
2.4
2.5
2.6
2.7
E_3 [GeV]
1.58
1.5
1.4
1.3
1.2
1.1
1.0
0.94
INVARIANT MASS [GeV]

FIG.3

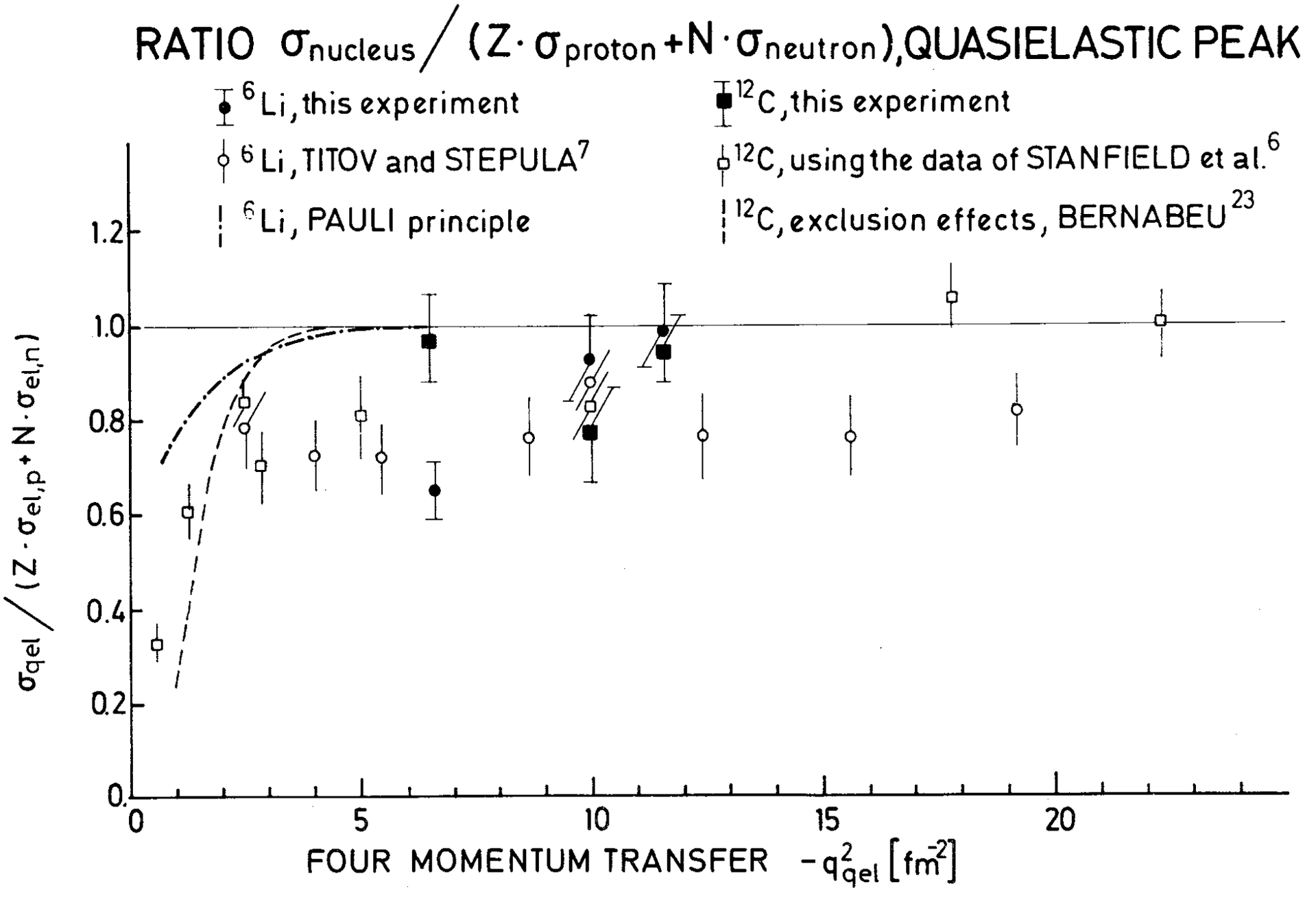
RATIO $\sigma_{nucleus} / (Z \cdot \sigma_{proton} + N \cdot \sigma_{neutron})$, QUASIELASTIC PEAK
^{6}Li, this experiment
^{6}Li, TITOV and STEPULA[7]
^{6}Li, PAULI principle
^{12}C, this experiment
^{12}C, using the data of STANFIELD et al.[6]
^{12}C, exclusion effects, BERNABEU[23]
$\sigma_{qel} / (Z \cdot \sigma_{el,p} + N \cdot \sigma_{el,n})$
1.2
1.0
0.8
0.6
0.4
0.2
0.
0
5
10
15
20
FOUR MOMENTUM TRANSFER $-q^2_{qel}$ [fm^{-2}]

FIG.4

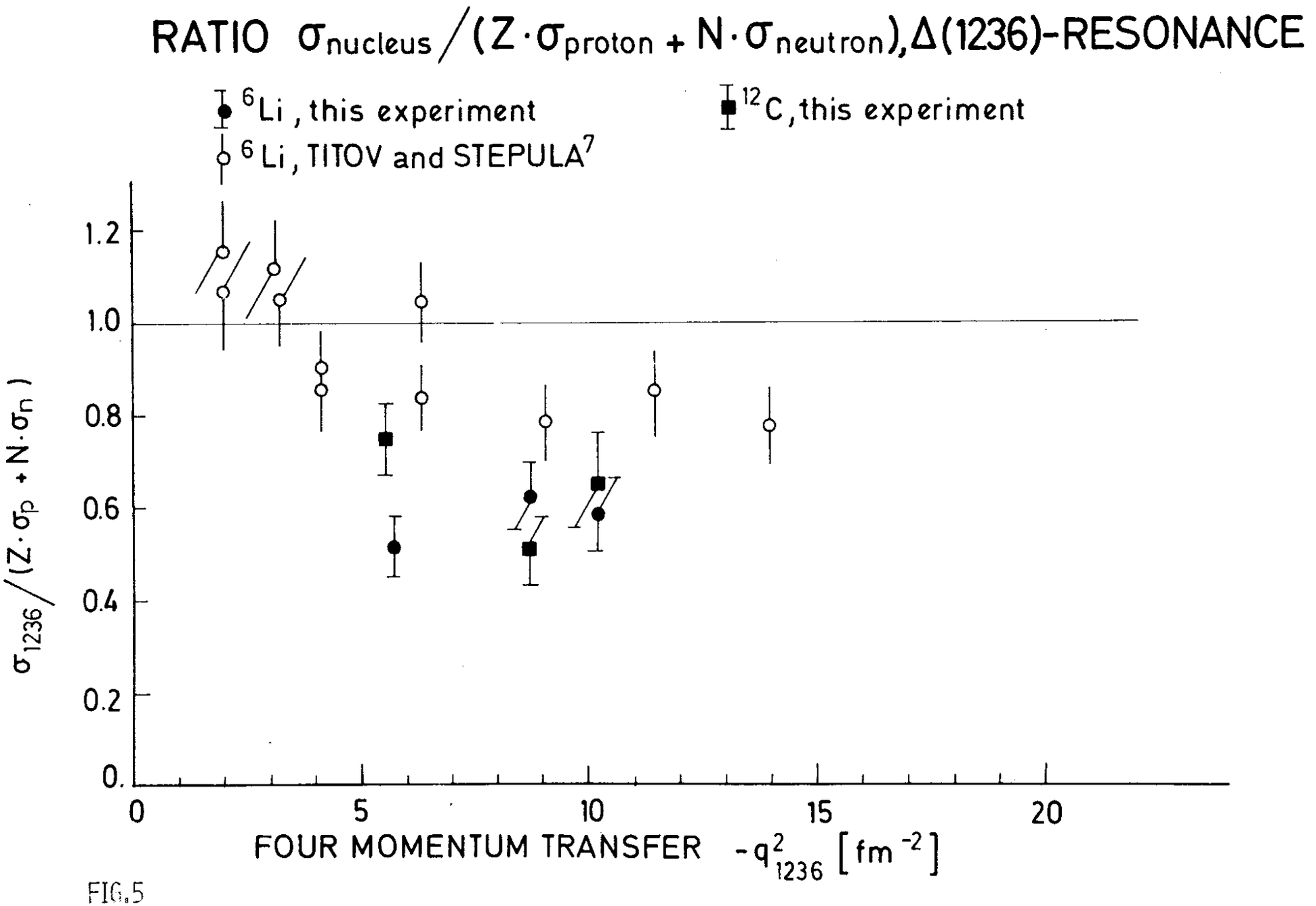
RATIO $\sigma_{nucleus} / (Z \cdot \sigma_{proton} + N \cdot \sigma_{neutron})$, Δ(1236)-RESONANCE
^{6}Li, this experiment
^{12}C, this experiment
^{6}Li, TITOV and STEPULA[7]
$\sigma_{1236} / (Z \cdot \sigma_p + N \cdot \sigma_n)$
1.2
1.0
0.8
0.6
0.4
0.2
0.
0
5
10
15
20
FOUR MOMENTUM TRANSFER $-q^2_{1236}$ [fm^{-2}]

FIG.5

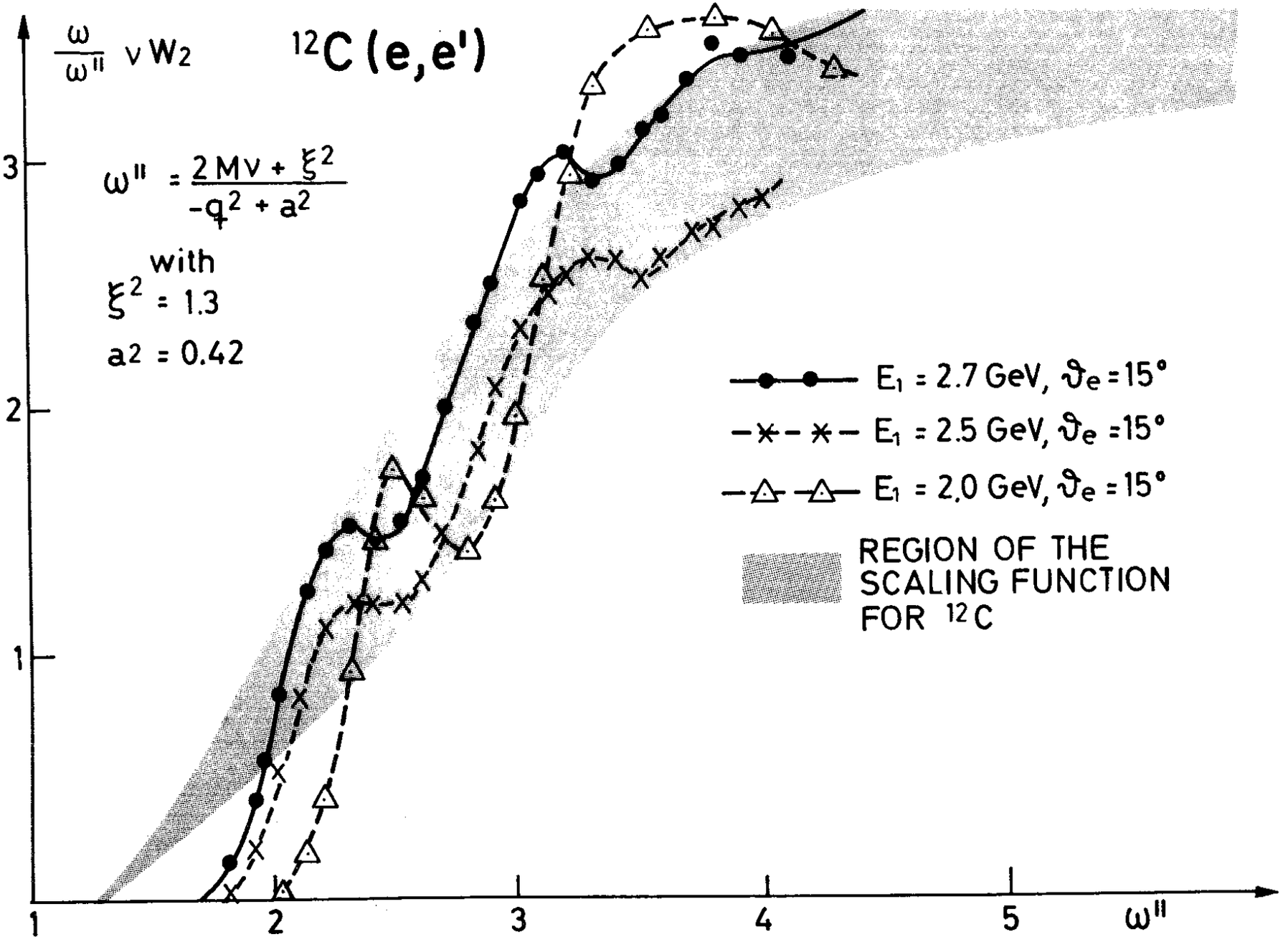
$\frac{\omega}{\omega''}\ \nu W_2$
$^{12}C\,(e,e')$
$\omega'' = \frac{2M\nu + \xi^2}{-q^2 + a^2}$
with
$\xi^2 = 1.3$
$a^2 = 0.42$
$E_1 = 2.7$ GeV, $\vartheta_e = 15°$
$E_1 = 2.5$ GeV, $\vartheta_e = 15°$
$E_1 = 2.0$ GeV, $\vartheta_e = 15°$
REGION OF THE SCALING FUNCTION FOR ^{12}C
1
2
3
4
5
ω''

FIG.6